INVESTIGATION OF CONTINENTAL DRIFT

Phase-II Effort

Contract NSR 09-015-079

Final Report

1 October 1968 through 15 March 1969

April 1969

Principal Investigator: Dr. Mario D. Grossi

N69-25155
ACCESSION NUMBER
52
PAGES
CR 108553
(NASA CR OR TMX OR AD NUMBER)
1
(CODE)
13
(CATEGORY)
FACILITY FORM 602

Prepared for
National Aeronautics and Space Administration
Washington, D C. 20546

Smithsonian Institution
Astrophysical Observatory
Cambridge, Massachusetts 02138

INVESTIGATION OF CONTINENTAL DRIFT

Phase-II Effort

Contract NSR 09-015-079

Final Report

1 October 1968 through 15 March 1969

April 1969

Principal Investigator: Dr. Mario D. Grossi

Prepared for

National Aeronautics and Space Administration
Washington, D. C. 20546

Smithsonian Institution
Astrophysical Observatory
Cambridge, Massachusetts 02138

904-59

TABLE OF CONTENTS

INVESTIGATION OF CONTINENTAL DRIFT

Phase-II Effort

Contract NSR 09-015-079

Final Report

1. SUMMARY

Stanley Ross

Our efforts during Phase II were concentrated on designing a plan for an initial very long baseline interferometry (VLBI) observation program to evaluate the accuracy of selected interferometer configurations. This approach is intended to provide a means for quantitatively examining the effectiveness of the interferometer technique for a variety of earth measurements. Special emphasis was applied to the following areas of investigation:

A) A screening of existing radio antennas to determine those most suitable for conducting the type of experimental program envisioned.

B) A preliminary analysis of the effects of major uncertainties on the accuracy achievable with a VLB interferometer.

C) For those sites of most interest, a check of available equipment for the acquisition, recording, and processing of the received signals.

D) An investigation of the adaptability of existing methods and instrumentation to the measurement of the columnar refractivity (atmospheric and ionospheric) along the ray path of the radio star.

E) A survey of natural and artificial radio sources to determine those most suitable for conducting the program.

F) Further investigations toward improving the data-processing capabilities at Smithsonian Astrophysical Observatory (SAO) for reducing the received signals.

G) Formulation of a draft plan for a schedule of observations to satisfy the study objectives.

Estimates of the time, manpower, equipment, and funding necessary to carry out the program are given in SAO's follow-on proposal for The Application of VLB Interferometry to Earth Measurements.

In formulating the observation plan, we stressed those aspects of VLBI that are appropriate to the measurement of continental drift, although consideration was also given to a number of other suggestions for earth measurements that the Phase-I study had identified.

From the list of candidate experiments we structured an initial program whose results should be applicable to many classes of earth measurements and whose scope should permit us to proceed further across a wide front if the results of the initial program are encouraging.

The conclusions of the study are the following:

1) The initial observation program calls for three major groups of measurements, the first being to conduct a precursor experiment to calibrate the SAO instrumentation over a short baseline in the Boston area; the second, to test the accuracy of the VLBI measurements against independently obtained data; and the third, to obtain fringes from a satellite-borne transponder in an attempt to study the design and operational problems of VLB interferometry using artificial sources.

2) Tropospheric and ionsopheric distortion of the radio-frequency signals remains the single most troublesome source of error, and simultaneous, direct probing still appears to be the only method of approach that can permit measurements to be made to an accuracy consistent with the requirements for detecting continental drift. We have placed increased emphasis on evaluating this technique in connection with the use of balloons at altitudes to perhaps 20 km.

The study identified several existing antenna facilities that would be suitable for the program we are contemplating. We visited most of these sites and spoke at length with personnel involved in the operation of the antennas. These individuals were in every instance generously hospitable and enthusiastic in support of our goals. In spite of this keen interest, however, many of the instruments are already heavily committed to a wide variety of other programs, and we have come to appreciate the extreme desirability of having at our disposal antennas that are freely available to our own program for the considerable amounts of time required. In this connection, it is our opinion that many of the capabilities represented within the existing National Aeronautics and Space Administration (NASA) tracking networks would be very well suited to a VLB interferometry program for earth measurements, and we have recommended that cognizant NASA officials give serious consideration to dedicating some of these instruments to the pursuit of such a program during slack periods in their schedules.

There also exist a few other sites at which the interest in participating in such a program is so strong that it would be advisable to give serious consideration to them as well. Of particular importance in this regard are the Vermilion River Observatory (VRO) in Danville, Illinois, at which a new 120-ft dish is being built by the University of Illinois, and the SAO-HCO (Harvard College Observatory) 84-ft Agassiz antenna at Harvard, Massachusetts. There are also many sites with smaller antennas of high quality, often readily available, to which it would be well to address ourselves, since the measurement of geophysical phenomena may have to be carried out at many sites where large antennas do not exist. The success of any program for measuring continental drift, for instance, may depend on how effectively we can employ small, perhaps portable, antennas at remote locations around the globe and it is important to begin to pursue this line of application as soon as the initial verification tests with large antennas have been completed.

The diversity of receiving equipment in use at different facilities was an important factor in shaping the details of the program, and the general unavailability of suitable high-bandwidth recording equipment heavily influenced the decision to build a transportable VLB back-end for our own use. In

considering the computational expense associated with the great quantity of measurements anticipated, we became aware of the necessity for building a digital correlator expressly for the program if costs are to be kept within reason. The correlator and the recording back-end will therefore have to be keyed to each other; the design of the two sets of equipment is a subject for our continuing research.

It is not our purpose to propose or develop new conceptual advances in instrumentation, but rather to adapt the program to equipment that is currently available off-the-shelf. Consequently, our choice of instrumentation for the VLB back-end was limited to readily obtainable hardware items of proved reliability. However, several new approaches have been started by a number of groups in an effort to increase recording bandwidths. Notable among these are the sampled-frequency multiplexer described by the Massachusetts Institute of Technology (MIT) Lincoln Laboratory (cf. Hinteregger, 1968), and the extended-bandwidth recorders currently under development by Ampex under National Radio Astronomy Observatory (NRAO) sponsorship and by Algonquin Radio Observatory (ARO) in Canada. These approaches should be capable of increasing the achievable bandwidth by at least an order of magnitude in the near future. Although such systems exist only in experimental form at present, we look forward to applying such new advances to the improvement of our own interferometer performance as soon as they become generally available.

We feel that the system we have specified for the preliminary measurement program should be capable of determining baseline length to an accuracy of some 50 m initially, and to somewhat better than half this amount at the next stage of refinement. This degree of accuracy will permit us to evaluate the sensitivity of the VLB technique, at least for the interferometer configurations adopted, and at the same time give us enough operational experience to choose the most effective means for improving the accuracy in subsequent phases of the study. Adopting a 50-m figure of accuracy for the initial measurements permits an interferometer of modest accuracy to be used for this phase of the program or, alternatively, it permits weaker radio stars to be used as source objects. We show below that stellar sources of about 5 to 10

flux units should suffice to give us measurements of the desired accuracy. Finding appropriate sources, therefore, does not appear to be a serious problem at this stage, and the matter becomes primarily one of choosing stars that are most favorably positioned relative to the adopted baselines. The problem of optimizing the choice of stellar-source position will be studied during the next phase of work.

Insofar as geological developments are concerned, evidence tending to support the existence of sea-floor spreading as a mechanism for producing continental drift has continued to accumulate, and we are including in the present report a summary of recent magnetic, seismic, and geochronological findings, pertinent to this study, that have come to light recently. Broad outlines are beginning to emerge of a system of global tectonics in close dynamic relationship to the rotation, precession, and wobble of the earth.

During the period since our last summary report, the SAO staff has been augmented by Drs. I. I. Shapiro and N. C. Mathur, whose contributions to our further efforts on this contract will play a significant role in accelerating the progress toward the study goals.

2. RESULTS OF RECENT GEOLOGICAL INVESTIGATIONS

Ursula B. Marvin

Evidence tending to confirm the reality of continental drift has continued to accumulate during the past half-year. The general concept of sea-floor spreading, with the generation of new crust along the oceanic ridges compensated for by crustal destruction at the deep trenches, is now supported by so many geophysical observations that the large-scale migration of crustal blocks, both oceanic and continental, seems no longer in serious doubt. Details of the model change as new measurements reveal special problems. The broad outlines are emerging, however, of a global synthesis in which many geological phenomena, including tectonic movements, magnetic reversals, and climatic fluctuations, are seen as interrelated and influenced by the dynamics of the rotation, precession, and wobble of the earth.

2.1 Magnetic and Seismic Data

To date, the pattern of sea-floor spreading has been outlined, on the basis of magnetic and seismic data, for about half of the world's oceanic area. The linear belts of magnetic anomalies paralleling the oceanic ridges have yielded evidence of 171 reversals of the geomagnetic pole during the past 76 million years, from the late Cretaceous to the present. A tentative magnetic time scale has been constructed by assigning ages to each successive anomaly belt. By this means "isochrons," or lines of equal age, ranging from 10 to 80 million years, have been drawn on ocean floor maps (see Figure 1, Heirtzler, 1968).

These isochrons indicate different spreading rates in different oceans and across separate ridge segments in the same ocean. The highest rates of spreading, ranging up to 10 cm per year, appear to have occurred across the East Pacific rise. In the Atlantic the spreading rates of about 2 cm per

Figure 1. Isochrons indicating ages deduced from magnetic time scale of belts of ocean floor. Numbers indicate ages in millions of years. Ridge segments: heavy black lines. Trenches: hachured lines. Isochrons: dashed lines with numbers. (From Heirtzler, 1968.)

year, deduced from the magnetic time scale, are in good agreement with those estimated from fossil and paleoclimatic evidence for the breakup of Gondwanaland and the separation of Africa and South America. Both lines of evidence suggest that the Atlantic is a young ocean that began to rift between 100 and 200 million years ago, in the Jurassic.

According to recent interpretations of seismic data from the oceanic ridges, the active slip occurs mainly along the planes between offset ridge crests and the direction of first movement indicates that these slip planes are indeed transform faults, as was predicted by Wilson (1965). Geometric analyses have demonstrated that the ridge-crest segments and their connecting transform fault lines tend to lie at right angles to one another and can be plotted upon a globe as longitudes and latitudes around a pole of spreading as shown in Figure 2. The poles of spreading are not the same for all oceans, and they apparently migrate with time for any one ocean. The present-day spreading poles for the Pacific Ocean and the South Atlantic are essentially identical and lie very close to the earth's magnetic poles. The poles of spreading deduced for these oceans in the Cretaceous lay close to the Cretaceous magnetic pole (Heirtzler, 1968). Thus, it appears that the gross pattern of earth movements is influenced by the same forces that govern the magnetic field with its changes in distribution, intensity, and polarity.

The ridge crests are extensional zones where sea-floor spreading is accomplished mainly by dike-like intrusions accompanied by shallow-focus earthquakes but relatively little effusive volcanism. The compensating destruction of crustal material occurs mainly in compressional zones along deep trenches and continental margins where the ocean floor is warped downward into the upper mantle. Most active volcanism and virtually all the world's deep-focus earthquakes occur along these zones, of which the Pacific margin is the prime example. Here the introduction of oceanic bedrock and sediments into the mantle may account for the andesitic petrology of the volcanic mountain chains rimming the Pacific Ocean (Dickinson and Hatherton, 1967).

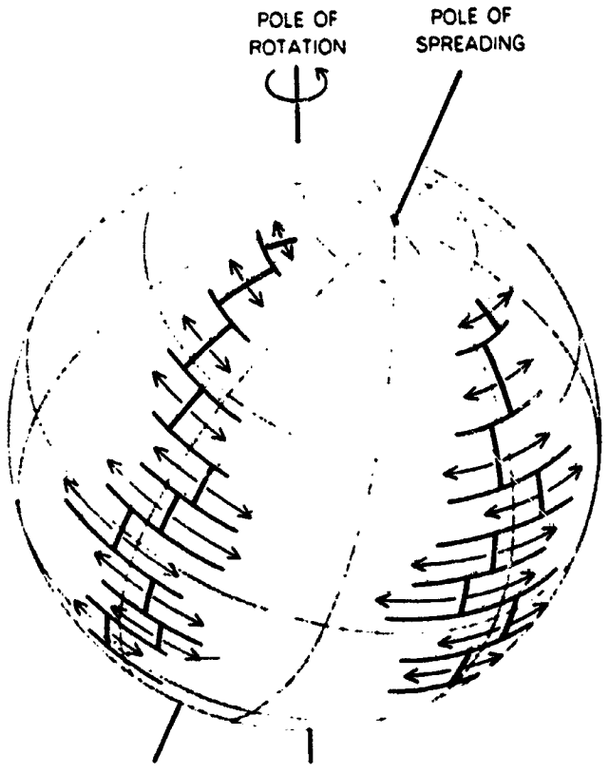

Figure 2. From Heirtzler (1968).

The absence of deep trenches and of volcanism along the Atlantic margins suggests that here the spreading sea floors are pushing continental masses ahead of them without immediate destruction of crust at the continental borders. If this is so, the spreading of the sea floor at the Mid-Atlantic ridge must involve crustal shortening in some distant part of the world. Indeed, the long-distance effects of earth movements are becoming recognized as an important aspect of global tectonics. A reinterpretation of seismic records suggests that crustal blocks are affected for thousands rather than only tens or hundreds of miles from earthquake epicenters. This view places individual earthquakes as events of global rather than local significance and validates the search for succeeding crustal movements halfway around the world (Press, 1965).

A striking correlation has recently been discovered between the occurrence of major earthquakes (Richter magnitude over 7.5) and changes in the Chandler wobble of the earth's axis of rotation. Reported by Smylie and Mansinha (1968), this correlation clearly suggests a causal relationship between earth movements and minor variations in the earth's rotation system.

The precession and wobble of the earth have also been credited with changes in the earth's magnetic field (Malkus, 1968) and with large-scale variations in climate accompanied by faunal extinctions. New observations tend to confirm the 30-year old, and formerly discredited, theory of Milankovitch that glacial periods are controlled by the insolation pattern resulting from precession (Broecker, Thurber, Goddard, Ku, Matthews, and Mesolella, 1968).

These new data and interpretations imply a geological/geophysical synthesis in which planetary diastrophism and the fluctuations of the geomagnetic field and of the earth's climate are seen as interrelated and governed, ultimately, by the dynamics of the earth's rotation.

2.2 Geochronological Results

In the past, one of the more effective criticisms of the continental-drift hypothesis as proposed by Wegener and DuToit was that it treated the Cretaceous-Tertiary continental breakup as unique and so accounted for only the latest episode of crustal deformation and orogeny among the many recognized in the geological record. In recent years, J. Tuzo Wilson has postulated the repeated opening and closing of the Atlantic Ocean and the movement of other continental masses in earlier geological periods. Recently, however, the results of an extensive program of dating of continental rocks by the K-Ar and the Sr-Rb methods have persuaded Prof. P. M. Hurley and his coworkers that the breakup of continental masses, initiated about 200 million years ago, was indeed a unique event and that there was no "pre-drift drift" (Hurley and Rand, 1968).

Radiation-age data on samples of basement rock are now available for about 68% of the continental area. These data indicate that the total extent of sialic crust was much smaller in the Precambrian and that the evolution of new crustal material has since been occurring at an accelerating rate: 45,000 m^2 per million years, 2,000 million years ago, to 120,000 m^2 per million years in recent earth history (Hurley and Rand, 1968).

When the Precambrian terrains are plotted on pre-Cretaceous-drift reconstruction maps, they tend to coalesce into two large shields of ancient rock bordered and embayed by belts of younger materials. This pattern seems an unlikely one if the Precambrian sialic masses originated and grew as several independent nucleii and then drifted together before the Jurassic period. It is Hurley's conclusion, therefore, that the ancient sialic crust formed and remained as two large, growing massifs until the Mesozoic, when some fundamental change in the earth's internal dynamics triggered continental drift. Tests are under way to determine how well paleomagnetic data support the details of this interpretation. Meanwhile, Alexander DuToit's postulated continents of Gondwanaland and Laurasia are revived or confirmed by the latest results from geochronology.

2.3 Stratigraphic Matching of Geosynclinal Basins: Brazil-Gabon

New data on the stratigraphy of the Propria geosyncline in Sergipe, Brazil, show a strong correlation with those on a geosyncline in Gabon, West Africa (Allard, Gilles, and Hurst, 1969). These two structural basins, now truncated by the Atlantic coastlines, appear as one unit striking Northwest-Southeast on the pre-Cretaceous reconstruction map of Bullard, Everett, and Smith (1965, Figure 3). In both structural basins, Jurassic rocks lie directly upon late Precambrian formations of similar lithology and metamorphic grade. The whole Paleozoic and early Mesozoic sections are missing. The Lower Cretaceous sections share similar sequences of nonmarine formations, similar hydrocarbon occurrences, several identical species of fossil fish, and 30 identical species of ostracods. In each basin, the Upper Cretaceous begins with a salt deposit that apparently marks the first

appearance of the [illegible] from the coast of either Sergipe or Gabon. The conclusion is inescapable that the basins originated as one landlocked structure and [illegible] the mid-Cretaceous, when rifting began between the regions of Africa and South America.

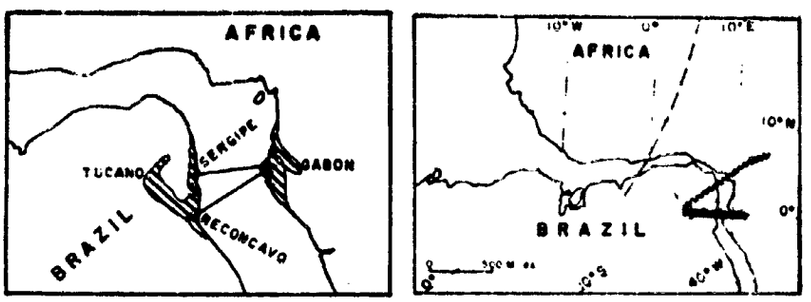

Figure 3A. Location map of Cretaceous sedimentary basins in Sergipe, Brazil, and Gabon, West Africa. 3B. Map of the continental margins as reconstructed by Bullard et al. (1965). Heavy solid line represents the location and trend of the Propria geosyncline in Brazil and its extension in Gabon; the jagged line follows the strike of mylonite zones in Brazil and the Cameroons; the dashed line locates a geochronological boundary within the Precambrian established by Hurley et al. (1967). (From Allard and Hurst, 1969.)

2.4 Conclusion

The weight of newly collected evidence supports the conclusion that crustal units are in motion at rates of 1 to 10 cm per year. Instrumental measurements of continental drift should, therefore, be fruitful. When the time comes to select sites for measurement, abundant geological information will be available for delineating the most active crustal zones.

3. OPERATIONAL CONSIDERATIONS AND INSTRUMENTATION

Stanley Ross and Richard D. Michelini

3.1 Test Plan

The initial test plan is intended to cover the period from July 1969 to July 1970. We emphasize that the facilities named below represent our best choices for implementing the program at this time but that, beyond purely exploratory discussions that we have held with them, no commitments have been made on their part or on the part of SAO for the use of the facilities. Pending the approval of the plan discussed in this report, SAO will move to establish formally such commitments with the cognizant authorities at these places.

Three major groups of experiment tasks are envisioned:

A) Task 1 is a precursor experiment to be conducted at L band over the short (8-mi) baseline between Haystack and Agassiz, using independent clocks at both stations. The goals of this experiment are to check out the Agassiz VLBI receiving and recording equipment and to acquire some degree of facility in the procedures involved in obtaining VLB fringes. This test has several favorable features to recommend it as a "learning" experiment:

- Haystack personnel have already conducted a number of VLBI experiments, and their participation in starting this program would be valuable to SAO.
- All the necessary equipment will be available at both sites for the test.
- Since both antenna sites are within the Greater Boston area, no extensive travel is required.

– There already exists an accurate ground survey between reference points at Agassiz and Haystack. This baseline can be used as a check against which to compare distance and directional information derived from the interferometer fringes.

B) Task 2 involves a series of tests at C band using the transcontinental baseline from Agassiz to the Owens Valley Radio Observatory (OVRO). Existing United States Coast and Geodetic Survey (USC&GS) surveys, combined with existing satellite data, are capable of tying Agassiz to OVRO via Edwards AFB or Goldstone to an accuracy of about 10 m, so that it should be possible to compare transcontinental baseline length and direction obtained by both methods to a significant degree of accuracy: about 50 m in baseline-length uncertainty is anticipated.

The 130-ft antenna at OVRO is mounted on four wheel-trucks that rest on a 250-ft east-west section of rails. It should be possible to move the antenna by measured amounts and then attempt to confirm this information by recovering the amount and direction of displacement from the fringe-derived data. The degree of agreement will give an indication of the sensitivity of the interferometer.

C) The Task 3 series has as its primary goal the acquisition of fringes from an artificial source – in particular, the S-band transponder from one of the Pioneer series space probes – and the comparison of baseline parameters obtained from this method against those already established in Task 2 both by ground/satellite surveys and by VLBI with natural radio sources. Perhaps most important, it will help us to understand some of the design and operational problems involved in satellite interferometry and thereby lend more strength to a study of design requirements for a satellite-borne interferometer source.

An Agassiz-Goldstone link is to be considered. This interferometer would be operated at S band because of Goldstone's commitment to the NASA Unified S-Band system. We have discussed with NASA the possibility of SAO's borrowing S-band receiving equipment; from these discussions, it appears likely that the equipment will be made available to SAO as needed.

The Agassiz-Goldstone link itself might even be established during Task 2. Involvement in the Task 2 transcontinental experiment would serve to establish the Agassiz-Goldstone baseline for Task 3.

3.2 Principal Sources of Error

We anticipate achieving an accuracy of 50 m in baseline length and about 10 μrad in baseline-to-star direction (both figures are order of magnitude).

Baseline parameters and stellar positions can be determined to an order of accuracy that is related to the size of the errors in the observables through the fundamental relationship

$$\lambda\Delta\phi = \vec{D} \cdot \hat{S} \quad , \tag{1}$$

where λ is the wavelength, $\Delta\phi$ is the phase difference in cycles, D is the baseline vector, and S denotes the stellar position. Differentiating, we find

$$\lambda\epsilon_{\Delta\phi} = \vec{\epsilon}_D \cdot \hat{S} + \vec{D} \cdot \vec{\epsilon}_S \quad . \tag{2}$$

When the baseline is perpendicular to the stellar-position vector, then $\vec{D} \cdot \hat{S} = 0$. Equation (2) shows that for this configuration the interferometer is insensitive to baseline-length errors; that is, $\vec{\epsilon}_D \cdot \hat{S} = \epsilon_D \vec{D} \cdot \hat{S} = 0$. This is certainly the case, since with such a configuration, each wavefront is received simultaneously at both stations, irrespective of the baseline length.

When the baseline is parallel to the stellar-position vector, $\vec{D} \cdot \hat{S} = 1$. Then $\vec{D} \cdot \vec{\epsilon}_S = 0$, since $\vec{\epsilon}_S \cdot \hat{S} = 0$. Thus, from equation (2), the more nearly D parallels $\hat{S}$, the less sensitive is the interferometer to errors in baseline-source direction.

Expressed qualitatively, this refers to the fact that if the baseline pointed directly toward the radio source, then any differentially small relative rotation (Figure 4) would cause the stations to move largely along the wavefronts on which $\Delta\phi$ is constant; that is, $\epsilon_{\Delta\phi} = 0$.

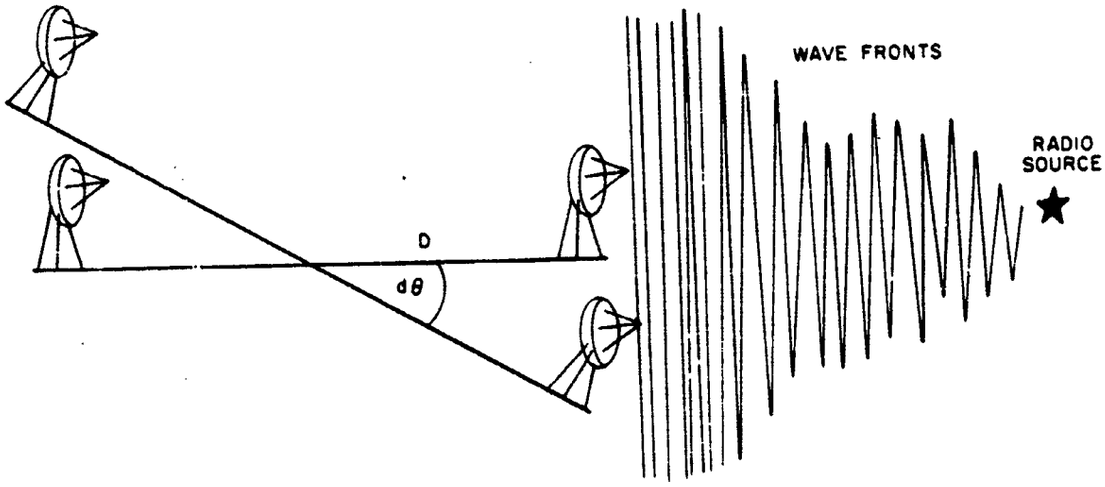

Figure 4. Baseline (D) pointing toward source.

Equation (2) can be rewritten as

$$c\epsilon_{\Delta t} = \vec{\epsilon}_D \cdot \hat{S} + \vec{D} \cdot \epsilon_S \qquad (3a)$$

or

$$c\epsilon_{\Delta t} = \epsilon_D \cos 0 - D\epsilon_S \sin 0 \quad , \qquad (3b)$$

where c equals the speed of light.

Significant timing errors are due to three principal causes:

- clock epoch-alignment errors at the two stations,
- long-term phase instabilities in the atomic standards, and
- bandwidth (or pulse-rate) limitations of the VLBI recording equipment at the stations.

An epoch-alignment error causes one clock to run late relative to the other. The signal then appears to be received slightly earlier at that station than it normally should be. This is identical to the effect produced by a slightly different baseline configuration. Equation (3b) shows that for the limiting case $0 = 0$, an $\epsilon_{\Delta t}$ in relative clock error produces an effect comparable to a change in baseline length of $c\epsilon_{\Delta t}$; for $|0| = \pi/2$, the effect is comparable to a baseline-direction change of $c\epsilon_{\Delta t}/D$. Thus, for these limiting cases, a 1-μsec epoch error is equivalent to a change of about 300 m in baseline length, or ± 300/D rad in baseline direction relative to the source.

The epoch error is constant with respect to time and can be treated as another unknown to be derived in terms of the observables by extending the observation schedule. Such a possibility has already been noted by several authors. In practice, of course, it is necessary to set the epochs close enough together so that fringes can be found without an undue amount of searching through the records; generally, an offset of 10^{-6} sec or better will suffice to produce fringes readily.

Over sufficiently long observation periods, phase instabilities in the atomic standards will also produce significant timing errors. Both rubidium-vapor and hydrogen-maser instruments have been considered for use in the VLBI experiments. Recent data (Cutler and Vessot, 1968) indicate that it is reasonable to adopt a stability figure of one part in 10^{12} for the long-term performance of rubidium-vapor standards; hydrogen masers are about 1.5 to 2 orders more accurate (Figure 5). Over a full day, then, the maximum accumulated time error with a rubidium standard can be expected to amount to 10^{-7} sec, which, from equation (3b), corresponds to an uncertainty of 30 m or more in baseline length, or ± 30/D rad in baseline direction.

A sufficiently high signal-to-noise ratio is required to achieve an acceptable degree of time resolution with the single-window, bandwidth-limited data channel planned for the measurements. The time resolution of

the system can be expressed in terms of the bandwidth and signal-to-noise (power) ratio as*

$$\epsilon_{\Delta t} \sim \frac{1}{(BW)\sqrt{S/N}} \cdot \frac{1}{\sqrt{\nu}} \quad , \tag{4}$$

where ν is the number of independent observations. In terms of equation (3b), a 50-m accuracy will require $\epsilon_{\Delta t}$ to be kept within about 0.15 μsec. From equation (4), then, the required value of S/N is about 25 for a single observation with a 1.2 MHz bandwidth, and $25/\sqrt{\nu}$ for ν observations

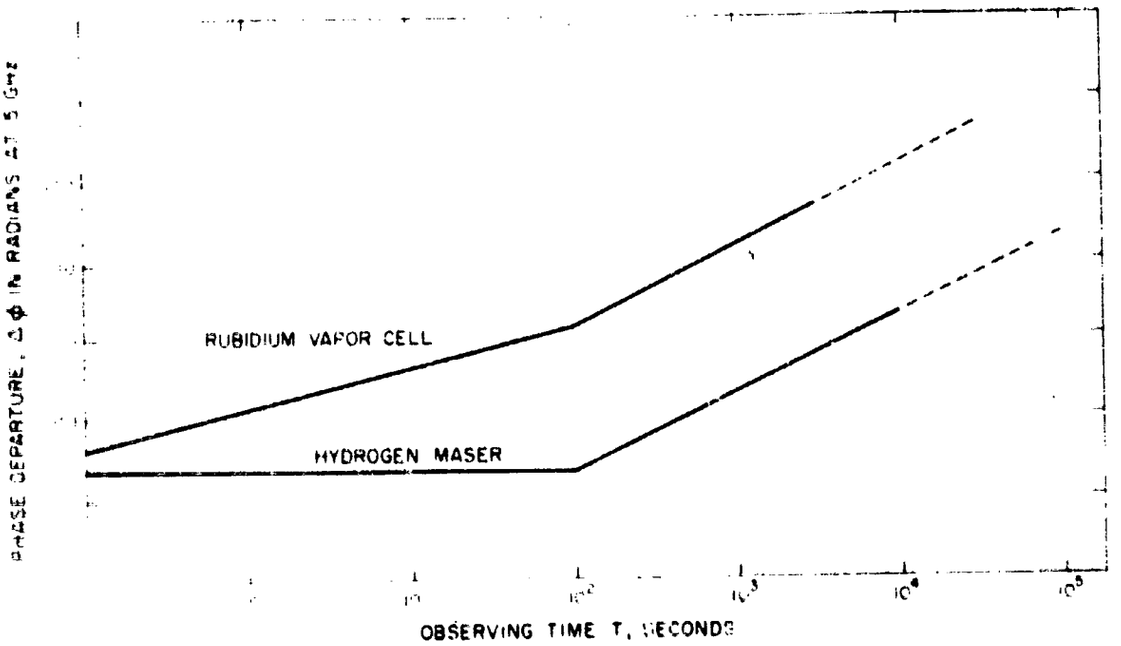

Figure 5. Phase departure vs. observing time.

*This assumes that the energy is constant across the spectral bandwidth (cf. Skolnik, 1962).

The signal-to-noise ratio for a pair of antennas x and y can be expressed (cf. Rogers, 1967) as

$$\frac{S}{N} = \sqrt{\left(\frac{T_a}{T_s}\right)_x \cdot \left(\frac{T_a}{T_s}\right)_y \cdot (BW) \cdot \tau} \quad , \tag{5}$$

where T_a is the antenna temperature, T_s is the system temperature, and τ is the integration time. Now T_a is expressible (cf. Kraus, 1966) as

$$T_a = \frac{S_0 A_e}{2k} \quad ,$$

where S_0 is the observed source flux density expressed in w/m^2 cps, A_e is the effective antenna aperture, and k is Boltzmann's constant (1.38×10^{-23} joule/°K). Substituting this last relation into equation (5) and rearranging terms, we have

$$S_0 = \frac{2k}{A_e} \left(\frac{S}{N}\right) \sqrt{\frac{(T_s)_x (T_s)_y}{(BW)\tau}} \quad \frac{\lambda^2}{D_x D_y} \quad , \tag{6}$$

where D_x and D_y are the antenna diameters (in meters at the operating wavelength λ).

Equation (6) relates the observed source flux density to the physical performance characteristics of the antennas and the instrumentation employed. For a given system bandwidth (which is usually appropriate for VLBI applications) and source, the ratio $S/N = 25$, and $BW = 1.2 \times 10^6$ established earlier, we find

$$S_0 = \frac{\sqrt{(T_s)_x (T_s)_y}}{D_x D_y} \quad 10 \text{ flux units}$$

(Note: 10^{-26} w/m^2-cps = 1 flux unit).

A range of typical antenna efficiencies, plotted as a function of operating frequency, is shown in Figure 6. Geometrical area multiplied by efficiency ϵ_{ap} yields the effective aperture area. To obtain an estimate of the minimum source strength required for the measurements, let us choose a pessimistic value of $\epsilon_{ap} = 0.2$ and adopt a value of 30 m as being representative of the geometrical dimension of the antennas to be used in the experiments. Then, $D_x \cdot D_y = 200$. Let us also adopt a value of $T_s = 250^\circ$ K as (conservatively) characterizing the systems to be used; S_0 assumes a value of about 13 flux units.

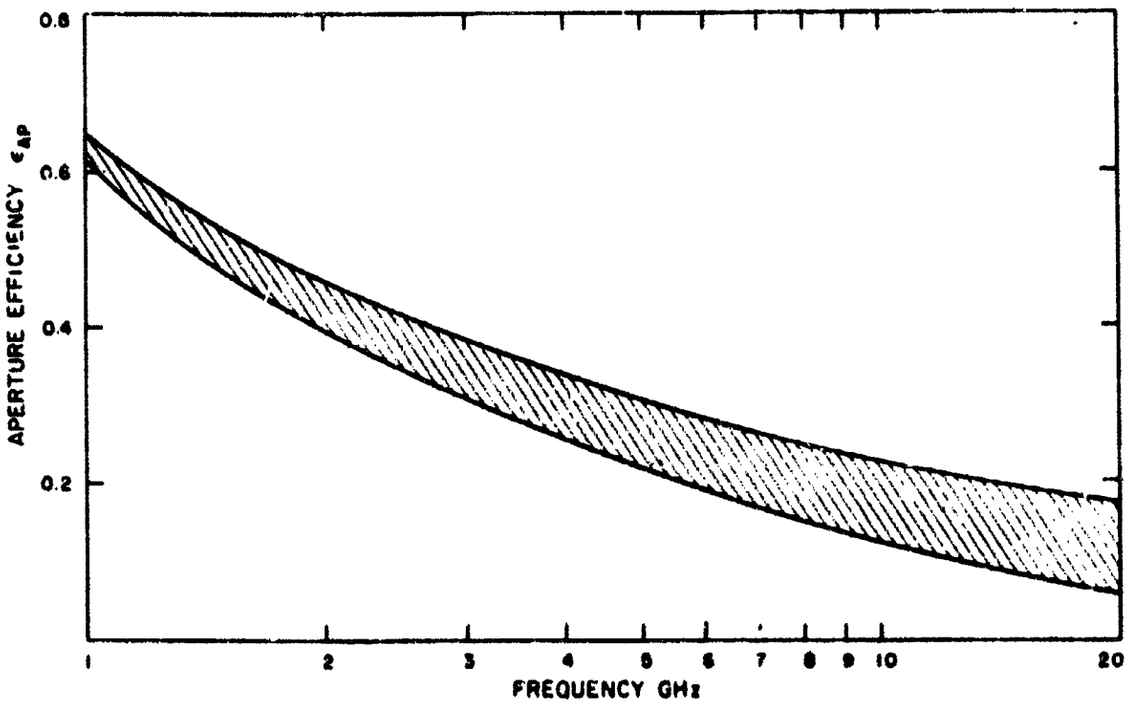

Figure 6. Range of typical antenna efficiencies vs. frequency.

Now, under more optimistic assumptions, with $D_x \cdot D_y = 400$, and $T_s = 165^\circ$K, S_0 assumes a value of about 4. We conclude, then, that source strengths of order 5 to 10 flux units should suffice for measurement

accuracies of 50 m with the systems discussed in this report. Thus, finding appropriate sources does not appear to be a very serious problem at this stage, and the matter becomes primarily one of choosing stars that are most favorably positioned relative to the adopted baselines. The problem of optimizing the choice of stellar-source position will be studied during the next phase of work.

In summary, then, the greatest uncertainty in timing appears to be due to epoch misalignment errors; however, these can be compensated for. Long-term phase instabilities and recording-bandwidth limitations should contribute an uncertainty of not more than about 50 m, and this figure might be reducible somewhat by exercise of due care.

3.3 Radio-Antenna Survey

The antenna survey concentrated on sites whose locations and operational conditions favored the goals of the experimental measurement program.

Four criteria were adopted to guide the site survey. We looked for installations at which there would be the following:

A) Relatively liberal availability of the equipment over the extended periods of time necessary to carry out the program.

B) Antenna sites whose distances and directions from one another are known (or can easily be determined) to an order of accuracy commensurate with the sensitivity of the interferometer system to be employed.

C) Moveable antennas on rails or two or more antennas located near one another. If a moveable antenna formed one terminal of an interferometer, then we could use it at two or more positions and attempt to confirm the measured changes in distance and direction by recovering this same information from the fringe data. Similarly, if each of a group of two or more closely spaced antennas in turn formed an interferometer terminal, attempts could also be made to confirm the relative distance vectors between them by means of fringe data.

D) An active interest on the part of the staff of the installation in participating in a geodetically oriented observation program.

After some preliminary investigation, we reduced the list of possibilities of five installations: Agassiz Station (HCO-SAO), Haystack (MIT-Lincoln Lab), OVRO (Cal. Tech.), Goldstone (JPL-NASA), and Vermilion River Observatory (University of Illinois). Table 1 summarizes some important characteristics of these facilities.

Agassiz (Figure 7a) seems to be the most desirable facility. Jointly administered by HCO and SAO, it is very readily available for the proposed program. Schedule complications appear to be minimal, which gives a great degree of flexibility to the program. Agassiz is also attractive because it is near SAO headquarters. Present receiving equipment is L band, but a C-band front-end on order will be available in time for use in the proposed program. At C band, the effective antenna diameter is expected to be about 34 ft. Performance of the pedestal drive is marginal but adequate for the present, if care is taken to use the antenna under relatively quiescent conditions.

At OVRO, there are three large antennas, all on rails: a pair of 90-ft dishes, and a new one of 130-ft diameter (Figure 7b). The former two are set on an L-shaped configuration of track, north-south and east-west, each leg extending 1600 ft. The 130-ft antenna is currently positioned on an east-west section of rail that extends about 250 ft. While the 90-ft dishes can be placed only at a number of discrete locations along each section of track, the 130-ft antenna can be positioned anywhere along its track. Cal. Tech. intends to extend the latter system of rails to a cruciform configuration having a 16,000-ft north-south leg bisecting a 9,000-ft east-west leg.

A first-order triangulation chain passes through Owens Valley (Lambeck, 1969), and the connection of the antennas into this net should be a minor task. From USC&GS data, the relative accuracy of the triangulation in the vicinity of both OVRO and Agassiz is estimated to be about 10 m in horizontal position

Table 1 Antenna sites under consideration

Facility	Location	Antenna	Receiving Equipment	Availability	Comments
Agassiz	Harvard, Mass.	1-? polar Fixed base.	L band; C band to be installed by summer 1969.	Excellent	Improvements to drive are planned but present one will be adequate for now.
Owens Valley	Big Pine, Calif.	1-.30' alt-az. On rails.	C band. Borrowed VLB back-end.	Good	Now scheduling usage for third quarter 1969.
		2-40' alt-az. On rails.	L band. No VLB back-end.	Poor	Mostly for student and staff research.
Haystack	Westford, Mass.	120' alt-az. Fixed base.	L band, X band. VLB back-end available.	Fair	Personnel experienced in VLB technique. Located close to SAO and Agassiz Station.
Goldstone	Goldstone Lake, Calif.	1-210' az. ring 4-85': 1 alt-az. 1 x-y 2 polar. All fixed base.	S band. No VLB back-end.	Probably only one (alt-az) avail. for research work.	JPL plans for VLB still uncertain.
Vermillion River Observatory	Danville, Ill.	120' polar. On rails.	L band (?). VLB back-end to be designed.	Excellent	Scheduled for operation fall 1969.

a) Agassiz Station (Harvard-SAO)

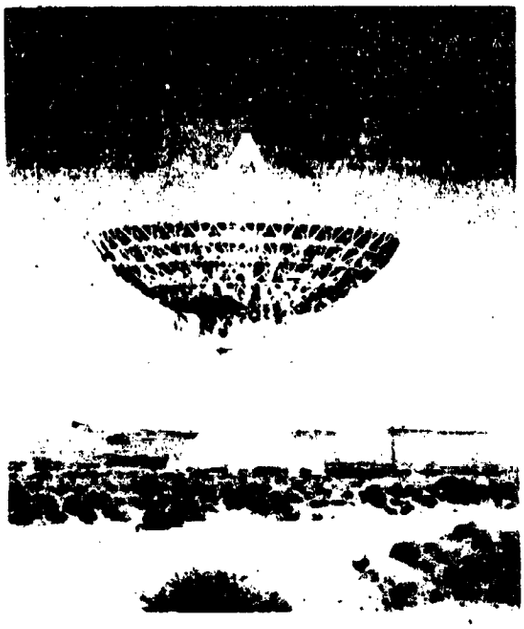

b) Owens Valley Radio Observatory (Cal-Tech)

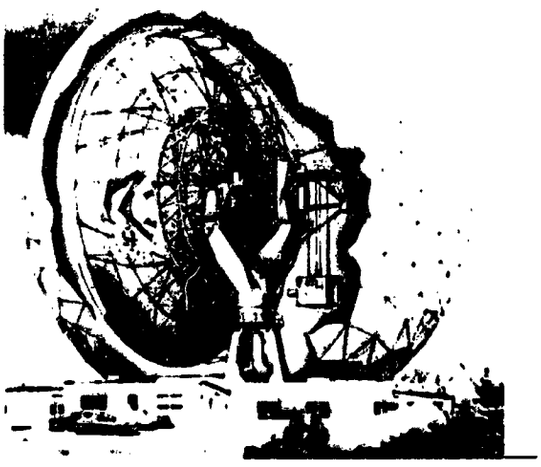

c) Haystack (MIT-Lincoln Lab)

d) Goldstone (JPL-NASA)

Fig. 7. Antennas.

and better than 5 m in elevation above the reference ellipsoid. Thus, the two sites can be connected via the survey with an accuracy that is comparable to that obtained between cameras 9113 (Edwards A.F. Baker-Nunn) and 9050 (Agassiz modified K-50) in the preliminary combination results of the dynamic, geometric, and Jet Propulsion Laboratory (JPL) data.

The Haystack Facility (Figure 7c) is of interest as a terminal in a preliminary experiment with Agassiz that could be used both to calibrate the Agassiz equipment and to permit SAO personnel to familiarize themselves with the operational procedures involved in operating a VLB interferometer. The prior utilization of this antenna for VLB work and the experience of Haystack personnel in this regard have already been noted. On the other hand, Haystack receiving equipment is limited to operation at L band and X band only, and the facility is not freely available on a regular basis, owing to its heavy schedule.

Goldstone has four 85-ft dishes and a fifth of 210-ft diameter, all operating at S band. Of the former four, two are equipped with polar mounts, one with an azimuth-elevation, and one with x-y. The azimuth-elevation instrument (Figure 7d) is the only one used for research-and-development work, the others being dedicated to flight-project applications. Goldstone is one of the sites from which Pioneer satellites are tracked, which is advantageous from the point of view of satellite-source interferometry (see Section 3.4). A Goldstone-Canberra VLB link using Pioneer 8 was achieved last year and was reported in the SAO Phase-I Report on Continental Drift. Goldstone can also be linked to Agassiz via existing ground and satellite surveys to about 10 m.

The University of Illinois antenna is currently under construction at VRO in Danville, Illinois. It will be of 120-ft diameter, on rails, and equatorially mounted. Prof. George Swenson, under whose direction the construction is proceeding, is personally very much interested in participating in a joint SAO-VRO program of geodetic measurements. Consequently, the antenna should be readily available to us. The largest drawbacks seem to

be in the uncertainty of the construction timetable, which makes it difficult at present to establish a specific experiment schedule, and in the antenna design, which may make it unsuitable for work at wavelengths shorter than 12 cm.

3.4 Artificial Radio Sources

Successful operation of a Goldstone-Canberra VLB interferometer using the S-band transponder on Pioneer 8 was noted in the Phase-I Report for the Continental-Drift Study. We investigated the possibility of using this satellite or another suitable one for a similar experiment. Three candidates were found: Pioneers 8, 9, and 10. The first two are currently in orbit, and the last is to be launched in June of this year, all in heliocentric orbits of about 1 a.u. The transponders operate continuously at a frequency of 2292 MHz; the signals are linearly polarized. Pioneer 8 was launched December 1967 into an orbit of 1.1 a.u. aphelion, and it now trails the earth somewhat. Pioneer 9 was launched November 1968 slightly inside the earth's orbit and is leading the earth. Signals from both probes are still being monitored; input power levels of -160 dbm from Pioneer 8 and -150 dbm from Pioneer 9 have most recently been measured at the 85-ft Pioneer dish at Goldstone, according to the Pioneer project office at NASA/Ames.

Pioneer 10 should be the most attractive of the three if it reaches its planned orbit, which will be almost identical to that of the earth. There should be a chance of tracking it for up to 12 hr per day, from horizon to horizon.

We also investigated the ATS synchronous satellites in orbit. Only ATS 1 and ATS 3 are viewable from the continental United States. The former is situated at a longitude of 150°W; ATS 3 is moved at various times between 47° and 90°W and is jointly viewable from Mojave and Rosman Stations. One major drawback is that the transmitter frequency of 4 GHz does not match the receivers available at the sites under consideration for the experiment program. No suitable ATS satellites are planned for the near future.

3.5 Instrumentation

The selection of radio-telescope sites to carry out the short- and long-baseline experiments will in part depend on the availability of instrumentation. Given a number of sites of suitable geographical location, each equipped with antennas that can be used to define the baseline distance, the quantity of instrumentation that must be provided by the experimenter has been a strong consideration in selecting an economical baseline. Included in the list of instrumentation are the terminal antenna; the radiometer, or so-called front-end; the data-frequency conditioning and recording equipment, or back-end; and the timing and frequency-control subsystems.

A principal requirement on each possible set of baseline antennas has been a moderately high signal-to-noise ratio. This is necessary to permit sufficient time resolution with the single-window, bandwidth-limited data channel planned for baseline measurements. Acceptable time resolution was shown to be achievable in Section 3 with S/N ≈ 25. Equation (5) showed the signal-to-noise ratio for a baseline pair of antennas x and y to be of the form

$$\frac{S}{N} \sim \sqrt{\frac{(T_a)_x}{(T_s)_x} \frac{(T_a)_y}{(T_s)_y} (BW)\tau} \quad ,$$

where T_a is the antenna temperature, T_s is the system temperature, and τ is the integration time.

Table 2 shows representative values of S/N calculated for the several experimental baselines. These values are based on an integration time of 100 sec and a bandwidth of 1.2 MHz. The source strengths used are representative of moderately strong nonresolvable sources; they range from 14 flux units of 1.6 GHz to 3 flux units at 5 GHz. Worst-case antenna efficiencies shown in Figure 5 were used in making the calculations. These

Table 2. Representative value of S/N for several experimental baselines

Baseline		1.6-GHz Experiment*			5-GHz Experiment†		
Antenna, a_1		$\frac{Ta_1}{Ts_1}$	$\frac{Ta_2}{Ts_2}$	$\frac{S}{N}$	$\frac{Ta_1}{Ts_1}$	$\frac{Ta_2}{Ts_2}$	$\frac{S}{N}$
Agassiz HCO-SAO 84-ft	MIT Haystack 120-ft	1/120	1/100	90	1/1150	1/580	12
Agassiz HCO-SAO 84-ft	OVRO 130-ft	1/120	1/60	120	1/1150	1/320	17

*Based on source of 4 flux units. Strength and integration time = 100 sec.

†Based on source of 3 flux units. Strength and integration time = 100 sec.

tabulated values indicate that the desired time-delay resolution can be attained with suitable margins allowed for instrumentation effects. Even with the combination of a relatively small antenna and high-temperature receivers, a S/N ratio of greater than 10 is possible.

In practice, the Agassiz-Haystack baseline will probably operate at 1.6 GHz so as to accommodate available receivers; however, the Agassiz-OVRO baseline will be used at 5 GHz, since instrumentation will be available at both sites for this frequency, and higher accuracy results are required.

3.5.1 Antenna-selection criteria

Discussions with the resident staffs of several observatories have been held during Phase II of this study to help select appropriate terminal sites. The 130-ft reflector at OVRO (Rule and Gayer, 1968) is expected to give good surface conformance (within $\pm 0.1\lambda$) at wavelengths down to 5 cm (the range from 1 to 6 GHz) Final surface adjustments may permit operation down to 2 to 3 cm. The large antenna will have about a 6.5-min beamwidth at C band, and the pointing accuracy will be a highly precise 20 arcsec.

Similar requirements are easily met or surpassed by the 120-ft Haystack dish and by several dishes at Goldstone and other NASA stations.

The 84-ft Agassiz dish has a surface accurate enough to provide tolerable aperture and beam efficiencies up to C-band frequencies. The previous limitation of pointing stability under wind loading will be removed by modifying the mount to hold a setting within 2 arcmin in winds of 25 mph. The dish is equatorially mounted.

3.5.2 Front-end requirements

The Agassiz terminal requires a C-band radiometer system roughly similar to that depicted in Figure 8. The basic components are the antenna feed, parametric amplifier, IF converters and amplifiers, and associated

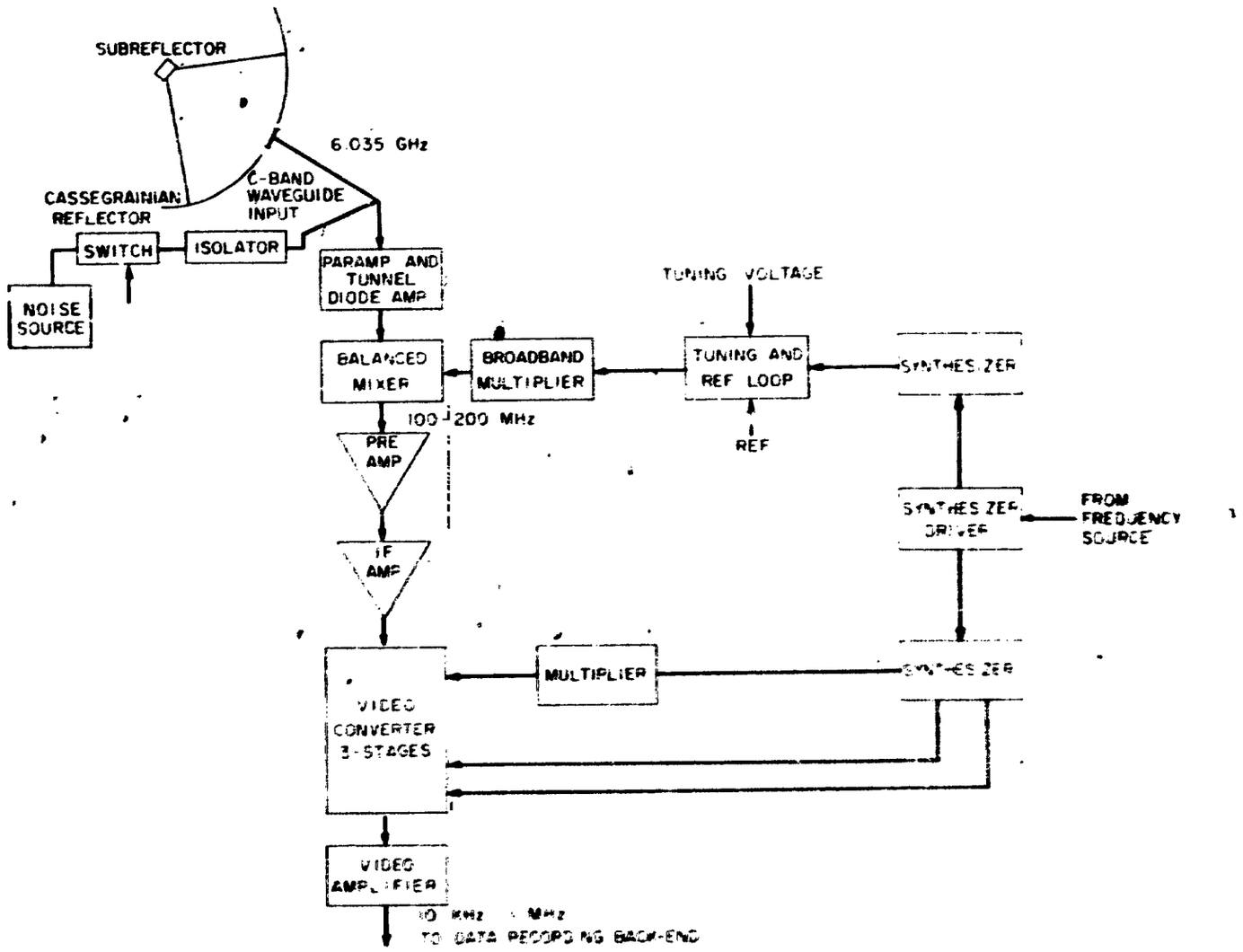

Figure 8. VLB receiver front-end for each terminal.

[illegible] oscillators. A linearly polarized feed and [illegible] will permit sufficiently low system temperatures [illegible] a variety of quasi-stellar sources [illegible] A noise source is included for meas- [illegible]

[illegible] front-end configuration can be [illegible] as sensitivity and noise figures [illegible] tunability covering [illegible] may conveniently coincide [illegible] and a video bandwidth as [illegible] relation. Linearity and [illegible] both receiver systems.

[illegible] acquiring and installing a suitable [illegible] requirements. It will be completed [illegible] alterations in the antenna-support [illegible] stability of the 84-ft Agassiz antenna will be [illegible] operations with Haystack, reception may have [illegible] interferometers at Haystack and Agassiz. However, [illegible] front-end can be installed at Haystack, using [illegible] radiometer.

[illegible] monitoring and recording subsystem

[illegible] monitoring and recording sys- [illegible] suitable equipment is currently available at [illegible] the most flexible and reliable plan will be to con- [illegible] properly packaged back-end assemblies that can be [illegible] in connection with the Agassiz facility. [illegible] readily into receiver systems at sites such as [illegible] Most of this specialized equipment is already [illegible] and are required for the construction [illegible] that includes the Haystack site.

The data-processing technique to be used is based on wide-bandwidth digital recording at the antenna sites, with playback, cross correlation, and fringe-phase processing performed at SAO in Cambridge. Figure 9 shows the processing system with a special-purpose cross-correlator to provide high-speed correlation of the site recordings.

A sampled-data, digital-recording technique (Rogers, 1968; Moran, 1968) is proposed for the generation of delay mapping data. This method is preferable to analog video recording with analog correlation (Yen, 1968) because it permits much easier time synchronization of the recordings and is more compatible with most existing VLBI terminals. With analog systems, precise time-base control of the video recorders is very difficult to achieve, even with expensive, high-quality quadrature recorders. Bandwidths up to 1.2 MHz are obtainable with the proposed digital recorders, and while this is somewhat below the maximum bandwidth that can be achieved with video recording, extension to higher bandwidths should be feasible with digital recorders that will soon be available. The precise frequency standards needed for independent-clock interferometry can easily supply the time-base stability required for the data digitizing.

The use of a special-purpose-channel digital correlator permits large quantities of data (up to 10^9 bits per observation period) to be reduced without requiring impractically long periods of processing time on a general-purpose computer.

The VLBI data-recording back-end (Figure 10) receives a signal derived from an intermediate IF stage and converts it into a filtered video signal, with a bandwidth of approximately 1 MHz. This signal is clipped and sampled at a 2-MHz rate derived from the timing system. The digital data are then shifted into a nine-track digital recorder. Various editorial formating is synchronously done in the form of record gaps and tape-drive signals. Time-synchronization data can also be placed on the tape records. Identical recording systems at each terminal will be capable of maintaining synchronization to within 1-bit resolution. Appropriate corrections to remove aliasing

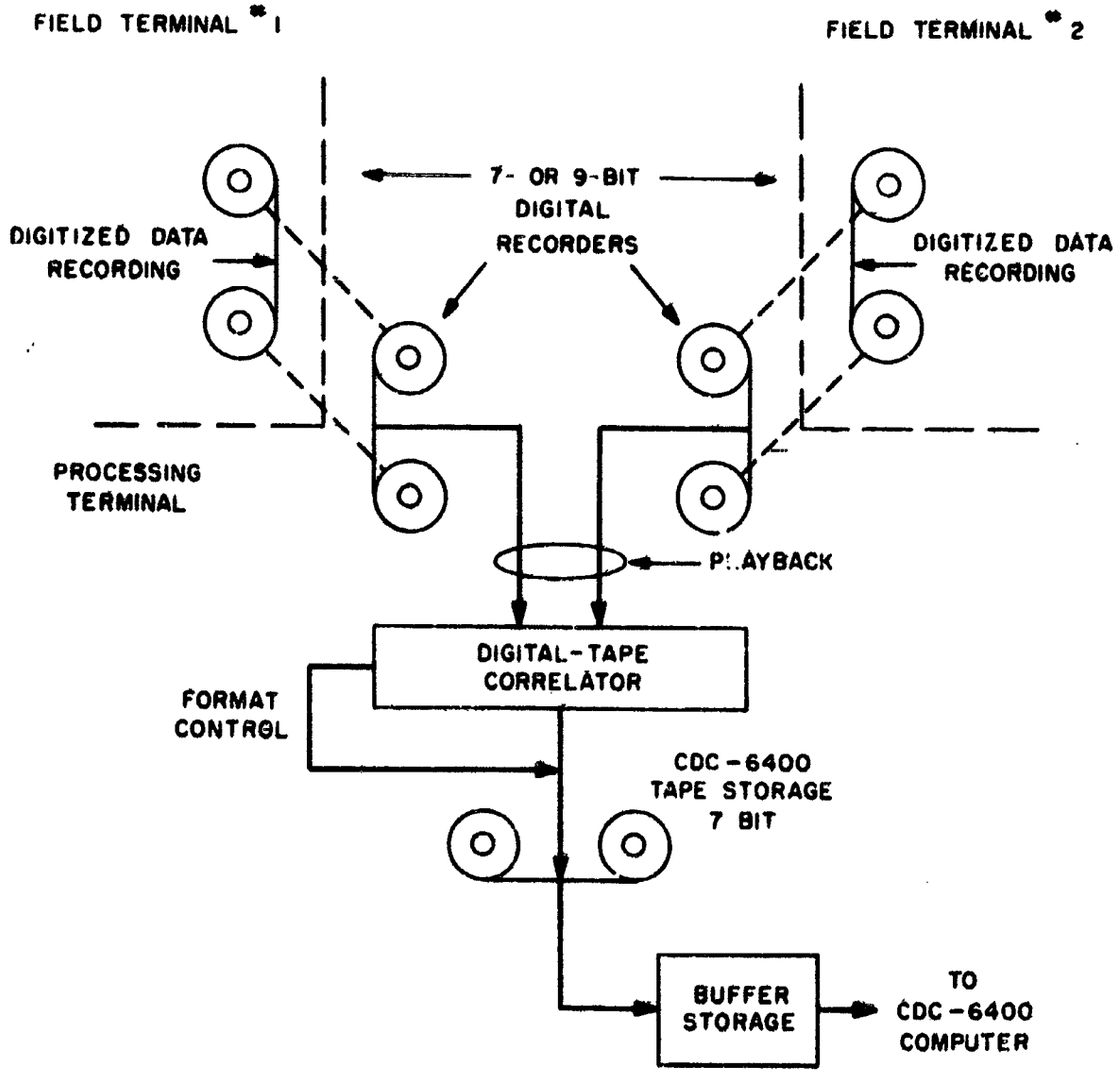

Figure 9. Data-processing schematic.

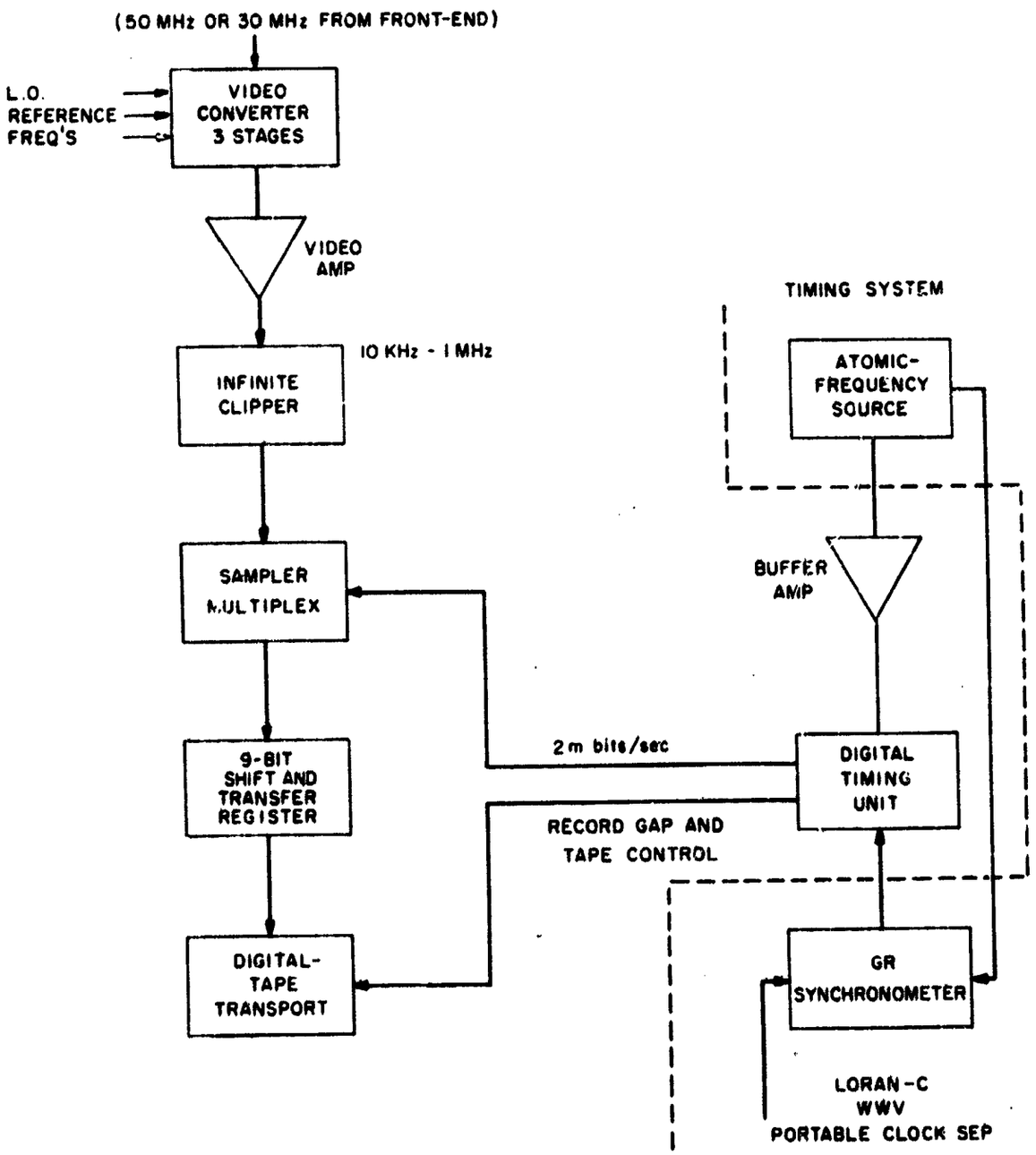

Figure 10. VLB data-recording band-end (each terminal).

error (from the bipolar sampling process) and to compensate for the finite sample size will be applied in the correlator. It should be noted that the timing base is locked to the same atomic-frequency source that drives the local oscillators in the front-end for the coherent conversion of the stellar radio signals.

Most of the equipment preceding the digital-tape transport shown in Figure 10 can be easily fabricated from commercial digital modules. To permit exploratory VLBI work to begin at minimum cost, we intend to rent the relatively expensive digital recorders; we can then more easily take advantage of future improvements in practical recording rates.

One possibility is to use as a correlator a specially programmed version of the H3 processor now being constructed by HCO-SAO under the Radio Meteor Project (Schaffner, 1966). This on-line processor will perform up to 16 delays over a sampling interval and provide single-bit correlation products at rates up to 2.5 MHz. Up to four accumulations can be executed in parallel. The use of this processor will reduce by a factor of 5 or 6 the general-purpose computer time needed for the project. More advanced versions of this processor will also be able to transform by fast Fourier analysis the correlation outputs and to compute directly the corrected delay times without the necessity of using a general-purpose computer.

3.5.4 Timing and frequency control

Each station requires an independent frequency source of the highest quality available. We plan to install a currently available rubidium-vapor frequency source (either a GTC Model 304B or 307B) at the western terminus of the long east-west baseline. Such a source will have a frequency stability of about 1 part in 10^{12} permitting the initial aspects of the baseline-confirmation experiment to be satisfied. The substitution of an improved source, such as a hydrogen maser, will result in an immediate increase in resolution and permit observations over periods of several hours.

A hydrogen maser may be available for the Agassiz facility. If it is not, a rubidium frequency standard similar to that mentioned above will be installed. Both rubidium units are currently available at SAO. At the Haystack site, a hydrogen maser (Varian Model H10) is already installed and accessible for VLBI applications.

Each station will also require a means of setting its clock to some coordinated time standard and maintaining synchronization with others. The maximum allowable time error must be such that the two digitized records can be matched bit by bit. If the first bit of each data stream is synchronized, succeeding bits will be matched without requiring continuous synchronization. Therefore, the relative time at two stations must be known to within a fraction of the reciprocal bandwidth ΔT. It should be noted that initial timing errors of several microseconds are acceptable (Cohen, 1968) since successive estimated delays can be applied to the data to achieve initial signal detection. If, however, the time synchronization is equal to ΔT, subsequent data tapes taken several hours apart can be correlated without a delay search.

The establishment of this degree of timing synchronization will permit traceability to a coordinated time standard [UTC(USNO), for instance] to within the accuracy required for stellar-position fixes and the solution of the baseline equations.

The requisite timing precision could be achieved by portable-clock trips from a master clock. However, terrestrial radio methods or satellite transponder transmissions would be a more convenient means of setting the clocks and checking clock drift. Most interferometer systems now use Loran-C navigation transmissions for time calibrations accurate of ± 1 μsec, using visual cycle selection. Resolution to 0.1 μsec is possible if automatic phase-tracking receivers are used (Shapiro, 1968). Such settings would be coordinated with the UTC (USNO) time scale.

For terminals such as Agassiz, Haystack, and those in the Midwest, a timing system based on Loran-C and portable-clock settings is satisfactory. Strong ground-wave reception from the Nantucket and Dana Point slave stations of the East Coast chain makes propagation uncertainties minimal. Figure 11 depicts such a system using a synchronometer as both an accumulator and a synchronous comparator. A phase-track receiver with visual selection is employed. Frequent calibration of the timing system will be done by means of portable quartz-crystal clocks circulating between the sites and the SAO master clock in Cambridge.

Unfortunately, reliable ground-wave reception of Loran-C radio signals is not possible at some West Coast sites. Consequently, a system of somewhat reduced accuracy, shown in Figure 12, will be used. Frequent portable-clock sets with a rubidium clock will be used to hold the station drift to within 2 or 3 μsec. This will be reduced to an uncertainty of 1 μsec by monitoring VLF station WWVL, which is extremely predictable diurnally over short, well-known paths. If possible, this system will also be augmented with a Loran sky-wave receiver, which is capable of producing similar accuracy.

Both these timing-system designs are based on past SAO timing experience and will utilize the coordinated facilities of the SAO master-clock station, which was established for synchronizing and defining time within the global SAO satellite-tracking network.

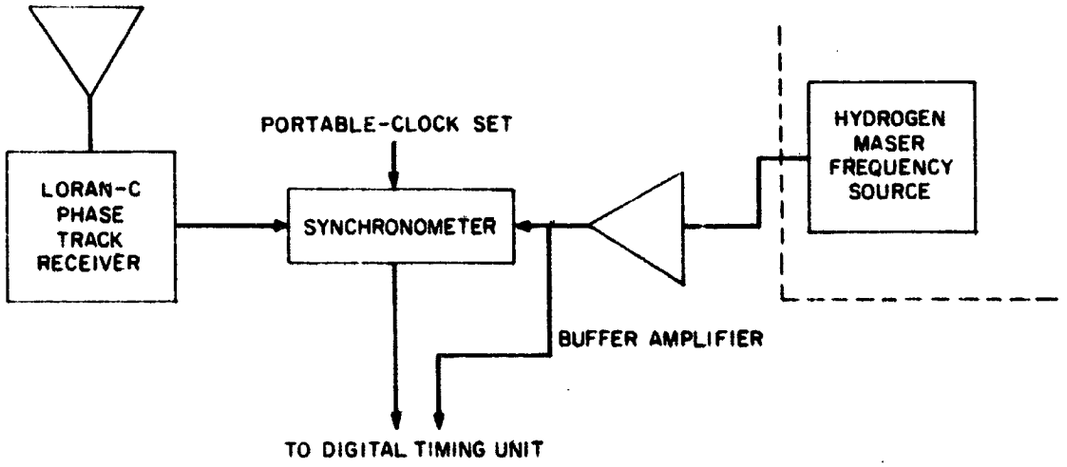

Figure 11. Timing system for Agassiz station terminal.

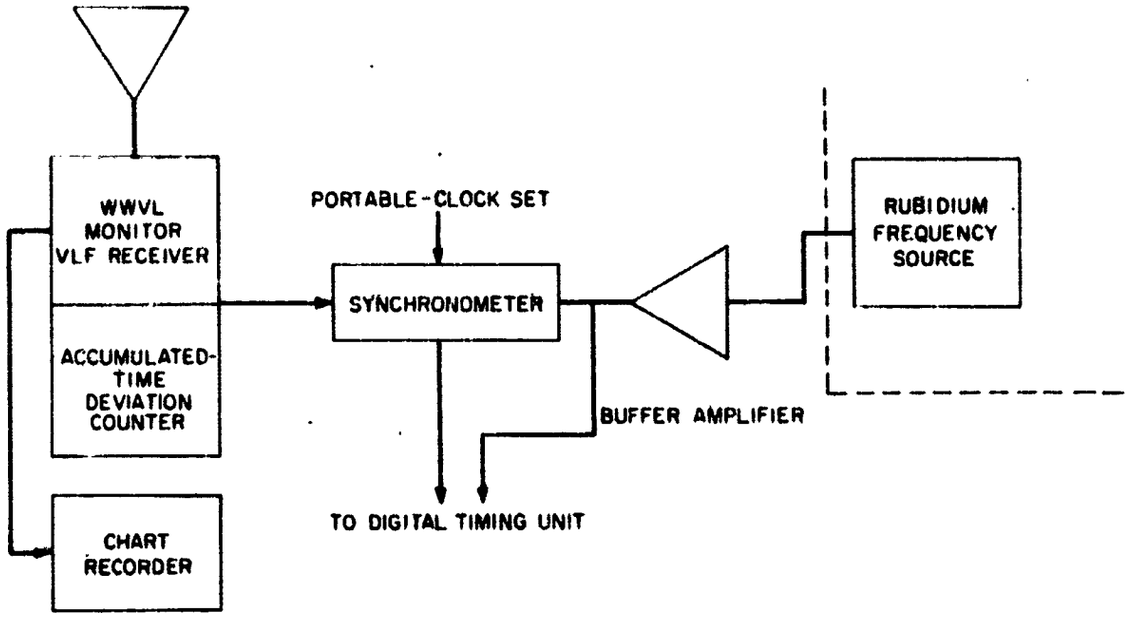

Figure 12. Timing system for West Coast terminal.

4. CORRECTIONS FOR TROPOSPHERIC AND IONOSPHERIC EFFECTS

Michael R. Pearlman and Mario D. Grossi

The measurement of the tropospheric and ionospheric perturbations that affect the proposed VLBI observations is a fundamental step in the attempt to meet the goals in baseline-length accuracy that are of interest to the geodesist and that are required for detection of continental drift. The use of models to estimate these perturbations is advisable only for the initial phases of the project when the accuracy goals are still modest.

The ultimate method must be a direct probing (at each terminal of the VLBI) of the troposphere and the ionosphere along the line of sight of the VLBI observations. The probing must then be done as nearly simultaneously as feasible with the VLBI observations.

If the ionosphere were the only plasma medium that had to be taken into account, the problem would not appear particularly difficult. One way of solving it would be to use X-band (10-GHz) or higher frequencies, where the ionosphere is transparent and the related correction terms are negligible. There remain, however, the column of electrons and its gradients in the interplanetary and interstellar regions between the radio star chosen for the VLBI observations and each terminal of the interferometer. Typical columnar densities of 10^{20} el/cm^2 characterize these paths, as compared to the 10^{12} el/cm^2 of the earth's ionosphere. This column introduces both a refractive "bias" and random fluctuations in the phase of the arriving wave front, effects that cannot be disregarded even at the X band. Recent measurements (Antonova and Vitkevich, 1968) show that these perturbations are measurable and that they are characterized by periods of 1 to 1.5 years. One would indeed expect periods of this length when the motion of the earth in its orbit and the consequent change in length of the column of electrons to the radio star are considered.

A way of removing this difficulty and of solving the problem of wave propagation in the various plasmas involved is to perform VLBI observations of the radio star at more than one frequency (Shapiro, 1969) and to measure the change in angle of arrival (angular motion of the interference fringes) from one frequency to the other. The assumption is that the ray paths at the two frequencies are close enough to each other to make this technique possible but still separated by a sufficient amount to make the diference in the apparent angle of arrival detectable.

For the tropospheric corrections, the measurements are more difficult and a continuing research effort is necessary in order to generate a workable approach. During the Phase-II study program, we evaluated the possibility of using atmospheric laser backscattering to provide the density profile of the troposphere along the direction of observations. However, the Mie scattering from dust aerosols was found to be comparable to the Rayleigh scattering from the air molecules. An approach using multicolor lasers with range-doppler-polarization measurement techniques would make it possible in principle to discriminate among the number densities of the various scatterers and to obtain the needed tropospheric columnar refractivity. However, since the instrumentation for this approach is quite complex, we are looking into an altogether different one. The system we are considering appears feasible, accurate, and less expensive; one or more balloons (powered, air-launched, or tethered) equipped with retroreflectors would be launched above the troposphere to points located along the direction of the VLBI observations. Maximum heights of about 20 km appear possible. The VLBI terminals would then be equipped with a three-frequency ranging system (two lasers and a C-band or X-band radar). From the differential group delays thus obtained, the columnar tropospheric refractivity could be derived, including the dry and wet terms.

Some work has been done with similar multifrequency techniques (Wood and Thompson, 1968; Owens and Earnshaw, 1968). These investigators have used the atmospheric dispersion to measure directly the columnar atmospheric refractivity along a path of interest. They measure the relative

phase delay of RF modulation on several optical and radio carriers (at different wavelengths) and reconstruct the atmospheric correction and the associated corrected path length.

Since the constituency of dry air is fairly uniform along any columnar direction, the index of refraction of the air N_{air} can be written in the form

$$\left| N_{air}(\lambda) - 1 \right| = \left[N_g(\lambda) - 1 \right] U(P, T) \quad , \tag{1}$$

where $N_g(\lambda)$ is the refractivity under standard conditions (15° C, 760 mm Hg, dry air, 0.03% CO_2) and $U(P, T) = P/T$ contains the pressure P and temperature T information and is accordingly an implicit function of altitude. The path-length difference between beams of two wavelengths λ_1 and λ_2 characterized by group indices of refraction $N_g(\lambda_1)$ and $N_g(\lambda_2)$ is given by

$$L_1 - L_2 = \left(N_{g_1} - N_{g_2} \right) \int_0^{S_0} U(P, T)\, ds \quad , \tag{2}$$

where s is the range along the path of interest. (Water vapor will be introduced later.) The phase delay along a given path through the atmosphere is then

$$L_1 - L = \int \left| N_{air}(\lambda_1) - 1 \right| ds = \frac{N_g(\lambda_1) - 1}{N_g(\lambda_1) - N_g(\lambda_2)} (L_1 - L_2) \quad . \tag{3}$$

Assuming a standard atmospheric constituency (0.03% CO_2), the index of refraction for dry air is given by the Edlén formula (Thompson and Wood, 1965):

$$\left[N_g(\lambda) - 1 \right] \cdot 10^6 = \left(64.328 + 29498.1 \frac{\left[146 + (1/\lambda)^2 \right]}{\left[146 - (1/\lambda)^2 \right]} + 255.4 \frac{\left[41 + (1/\lambda)^2 \right]}{\left[41 - (1/\lambda)^2 \right]} \right) , \tag{4}$$

while $L_1 - L_2$ can be measured by the modulation-phase comparison network. Since the dry-air atmospheric dispersion is very large in the optical region, we recommend two widely separated optical wavelengths (red and violet) for the dry-atmosphere propagation correction.

Deviation from the standard air constituency will slightly affect the dry-air dispersion relations, but even with CO_2, which will probably introduce the largest uncertainties, a factor of 3 or 4 increase in total content will only introduce a ranging error of 1 mm at zenith (Thayer, 1967). The sensitivity of $L_1 - L$ to variations in $L_1 - L_2$ is

$$\delta(L_1 - L) = \frac{N_g(\lambda_1) - 1}{N_g(\lambda_1) - N_g(\lambda_2)} \delta(L_1 - L_2) = \frac{1}{a} \delta(L_1 - L_2) \quad . \tag{5}$$

The dispersion across the optical region gives an a of about 0.1, and

$$\delta(L_1 - L) \approx 10 \delta(L_1 - L_2) \quad . \tag{6}$$

The range delay error due to the unaccounted presence of water vapor has been calculated (Thompson and Wood, 1965) and is tabulated in Table 3 for a 10-km horizontal path. The case along the zenith can be approximated by considering an average vapor pressure over the first scale height of the atmosphere (8 km).

[illegible] Range Error (Thompson and Wood [illegible])

Temp.	H_2O Vapor Pressure	Total Range Error
[illegible]	(mm Hg)	(cm)
[illegible]	[illegible]	0.4
[illegible]	[illegible]	0.8
[illegible]	[illegible]	1.7
[illegible]	[illegible]	2.8
[illegible]	[illegible]	4.6
[illegible]	[illegible]	8.4

In the [illegible] estimate of the water vapor to within 10% will allow [illegible] under the most adverse conditions. Systems [illegible] water vapor [illegible] developed (Wood and [illegible]) [illegible] propagation [illegible] caused by water vapor [illegible] radio frequencies could [illegible] used (relying on the lack of [illegible] in the radio region), but the optical-to-radio frequency [illegible]

The water [illegible] of the radio frequency index of refraction is dominated [illegible] water vapor term [illegible] $W(\ldots)$, and

$$[\text{illegible}] \qquad (\ldots)$$

where

$$N_c(\lambda) = N_g(\lambda) - 1$$

for this case. Thayer (1967) has solved the three-frequency system equations for a horizontal propagation path and obtained the atmospheric delay as a function of the measured path difference. His results take the form

$$L_3 - L = B_1 \left(1 + \frac{\Delta B_1}{B_1} \overline{T}\right)(L_2 - L_1) + B_2 \left(1 + \frac{\Delta B_2}{B} \overline{T}\right)(L_3 - L_1) \quad , (8)$$

where B_1 and B_2 are constants related to the wavelengths used in the system, and $\overline{T}$ is the average temperature over the path. For a system containing $\lambda_1 = 6943$ A, $\lambda_2 = 3660$ A, and λ_3 = several centimeters, Thayer finds

$$L_3 - L = 10.6642 (1 - 3.00 \quad 10^{-6} \overline{T}) (L_2 - L_1) - 1.02135 \left(1 + \frac{0.07465}{1.02135} \overline{T}\right)(L_3 - L_1). \quad (9)$$

The radio atmospheric correction is an order of magnitude less sensitive to variation in $(L_3 - L_1)$ than it is to those in $(L_2 - L_1)$.

For a vertical path under conditions that require the three-frequency technique for accuracy, some method will have to be found to handle the temperature dependence introduced by the polar water-vapor term. Since the scale height of the water vapor is only a few kilometers, low-altitude temperature profiles may be sufficient to obtain reasonable results. Considerable evaluation is still required to test the feasibility of the three-wavelength system as a probing technique through the atmosphere and then to test the accuracies at which such a system could operate.

We are considering a two-frequency radio-interferometer experiment in which the dispersion of the ionosphere and interplanetary electrons will be used to handle the phase delays caused by these media (Shapiro, 1969). This system would account the [illegible] a second microwave frequency for ionospheric corrections [illegible] Thayer, 1967).

The multiple [illegible] ranging technique described here does not account for [illegible] path lengths). Besides, turbulence may [illegible] each path in a different manner. Optimum operation [illegible] will be limited to conditions where the various paths [illegible] are geometrically coincident.

The optical instrumentation for the two-frequency atmospheric-correction system has been developed by Thompson and Wood, and others. Although it has only been used between surface-based terminals, there appears to be no obvious obstacle to using the system with a balloon-borne terminal or retroreflector. The simplified general system is shown in Figure 15. Details of such systems are dealt with at length by several authors (Wood and Thompson, 1968; Owens and Earnshaw, 1968). These optical ranging devices have been used over path lengths of 65 km and appear to have the capability of operating over much longer ranges with some modifications, but the tracking capability will require some special effort.

Referring to Figure 15, the path length difference between λ_1 and λ_2 is

$$L_1 - L_2 = \frac{\phi_1 - \phi_2}{2\pi} \lambda \quad ,$$

where λ is the modulation wavelength given by $\lambda = c/f$. The two channels must be calibrated to remove any systematic error. Phase-comparison networks do exist that are capable of discriminating phase differences of less than 10^{-3} wavelength. According to Owens at Environmental Science Services Administration (ESSA) (private communication) optical modulators capable of operating at 100 MHz are reasonable, and so we could expect to achieve a system sensitivity of a fraction of 1 cm [see equation (6)].

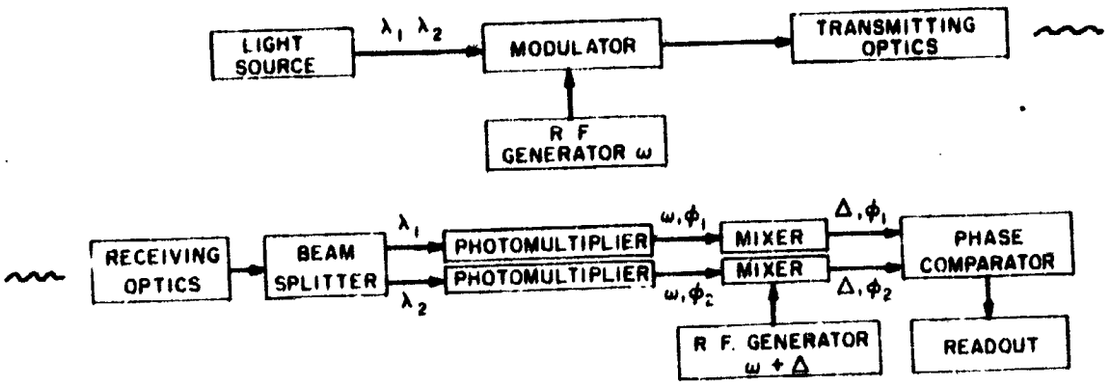

Figure 13. Block diagram of probing system.

The addition of a third frequency (microwave band) to the system is straightforward and has been already performed successfully by Wood and Thompson at ESSA (private communication). For our application, the third frequency could be provided by a radar working in the X-band region, and it is conceivable that the microwave carrier could be used as modulation for the optical frequencies.

The approach described above is capable of measuring the propagation delay through the atmosphere and can easily be adapted for absolute range measurements. Frequency or amplitude coding can be added to one of the transmitted beams (either optical or microwave) to enable us to make absolute time-of-flight measurements. Thompson and Wood have a modulation frequency-shift technique (to take ranging data) that could also be directly applied to our system.

At a height of 15 km, 85% of the atmosphere and essentially all the variability are below the balloon, and a good differential-phase path measurement should reduce the atmospheric propagation delay error to centimeters.

For the optimum system, the balloon must track the radio star across the sky. Angular separation should be no larger than is required to run both radio and atmospheric operations simultaneously. Radio-interferometer measurements will be taken over short intervals (several minutes), where stellar motion will be limited to about 1 . We will investigate the possibility of tracking for longer periods with powered balloons, by utilizing the prevailing winds or by relying on multiple-balloon arrays. For a single- or multiple-balloon system positioned within 1° of the line of sight of the radio star, the columnar probe is at most a fraction of 1 km from the radio observation path (0.25 km at 15-km altitude). Thompson at ESSA (private communication) has shown that the columnar phase delays over paths separated by 2 km are very well correlated , but this will have to be verified. Refractive bias may differ only negligibly over paths so close, but variability could limit our experimental accuracies.

Rather than carry large amounts of equipment aboard the balloon, we would use an optical retroreflector and do both the laser transmitting and detecting at the ground station. The microwave operation will probably require that some detection and transponder equipment be air-borne. A balloon-borne retroreflector is also usable for the radar.

For the case where continental-drift measurements are attempted by satellite-tracking techniques instead of by VLBI radio-astronomical approaches, the tropospheric and ionospheric corrections can be obtained more readily. For the satellite-tracking system, the satellite itself could be used as the target carrying the transponder or receiver. This is the ultimate in experimental technique (measuring the correction over the entire path by the four-frequency technique). The problems of range and tracking must, of course, still be surmounted.

5. REFERENCES

ALLARD, O., and HURST, V. J.

1969. Brazil-Gabon geologic link supports continental drift. Science, vol. 163, pp. 528-532.

ANTONOVA, T. D., and VITKEVICH, V. V.

1968. Results of radioastronomical investigations of heterogeneities of interplanetary plasma from data for 1965–1966. Astronomicheskii Zhurnal, vol. 45, no. 5, pp. 991-1001.

BARRELL, H.

1951. The dispersion of air between 2500 Å and 6500 Å. Journ Opt. Soc. Am., vol. 41, pp. 295-299.

BROECKER, W. S., THURBER, D. L., GODDARD, J., KU, T.-L., MATTHEWS, R. K., and MESOLELLA, K. J.

1968. Milankovitch hypothesis supported by precise dating of coral reefs and deep-sea sediments. Science, vol. 159, pp. 297-300.

BULLARD, E., EVERETT, J. E., and SMITH, A. G.

1965. The fitting of the continents around the Atlantic. In a Symposium on Continental Drift, Phil. Trans. Roy. Soc. London, vol. 258, pp. 41-51.

COHEN, M. H., JAUNCEY, D. L., KELLERMANN, K. I., and CLARK, B. G.

1965. Radio interferometry at one-thousandth second of arc. Science, vol. 162, pp. 88-94.

CUTLER, L. S., and VESSOT, R. F. C.

1968. Present status of clocks and frequency standards. NEREM Records, pp. 68-69.

DICKINSON, W. R., and HATHERTON, T.

1967. Andesitic volcanism and seismicity around the Pacific. Science, vol. 157, pp. 801-803.

HERTZLER, J. R.

1968. Sea-floor spreading. Scientific American, vol. 219, no. 6, pp. 60-70.

HINTEREGGER, H. F.

1968. A long baseline interferometer system with extended bandwidth. NEREM Record, pp. 66-67.

HURLEY, P. M., and RAND, J. R.

1968. Radiometric age data on two-thirds of the continental area of the Earth, Abstract. Geol. Soc. America 1968 Annual Meeting. Mexico City, pp. 145-146.

KELLY, T. W., Ed.

1967. Proceedings, AFCRL Tethered Balloon Workshop. Aerospace Instrumentation Laboratory, AFCRL, Office of Aerospace Research, U. S. Air Force.

KRAUS, J. D.

1966. Radio Astronomy. McGraw-Hill Book Co., New York, p. 99.

LAMBECK, K.

1969. Radio telescope at Owens Valley and Agassiz. SAO memo to E. M. Gaposchkin, January 30.

LEHR, C. G., MARVIN, U. B., and MOHR, P. A.

1968. Investigation of Continental Drift. Phase-I Effort. Contract NSR 09-015-079. Smithsonian Institution Astrophysical Observatory, Cambridge, Massachusetts.

MALKUS, W. V. R.

1968. Precession of the Earth as the cause of geomagnetism. Science, vol. 160, pp. 259-264.

MORAN, J.

1968. Ph. D. Thesis, Dept. of Electrical Engineering, Research Laboratory for Electronics, Massachusetts Institute of Technology.

OWENS, J. C., and EARNSHAW, K. B.

1968. Development of a Microwave Modulation Frequency Dual Optical Wavelength Geodetic Distance Measuring Instrument. Final Report for Research Institute for Geodetic Science. U. S. Army Engineer Topographic Laboratory, Fort Belvoir, Virginia. Task II, September.

PRESS, FRANK.

1965. Displacements, strains, and tilts at teleseismic distances. Journ. Geophys. Res., vol. 70, pp. 2395-2412.

ROGERS, A. E. E.

1967. The Haystack-Millstone interferometer. MIT, Research Laboratory for Electronics Tech. Rep. 457, March 15.

1968. Spectral line interferometry and interferometer noise analysis. Tech. Rep. 441, Lincoln Laboratory - MIT, Lexington, Mass.

RULE, B., and GAYER, G. F.

1968. A new radio telescope for the Owens Valley Observatory. Westinghouse Engineer, November, pp. 162-167.

SCHAFFNER, M. R.

1966. The circulating page-loose system - A new solution for data processing. Smithsonian Astrophys. Obs. and Harv. Col. Obs., Radio Meteor Project Research Report No. 15 (December). Contract No. NSR 09-015-033.

SHAPIRO, I. I.

1969. Lecture on VLBI at the Harvard College Observatory, January 23, 1969.

SHAPIRO, L. D.

1966. Time synchronization from Loran-C. IEEE Spectrum, pp. 46-56. (August).

SKOLNIK, M. I.

1962. Introduction to Radar Systems. McGraw-Hill Book Co., New York, pp. 4-63.

SMYLIE, D. E., and MANSINHA, L.

1968. Earthquakes and the observed motion of the rotation pole. Journ. Geophys. Res., vol. 73, pp. 7661-7673.

THAYER, G.

1967. Atmospheric effects on multiple frequency range measurements, ESSA. Tech. Rep., IER56-ITSA53 October.

THOMPSON, M. C., and WOOD, L. E.

1965. The use of atmospheric dispersion for the refractive index, correction of optical distance measurements. Electronic Distance Measurement Symposium, Oxford, Sept. 1965.

WILSON, J. T.

1965. Transform faults, oceanic ridges, and magnetic anomalies southwest of Vancouver Island. Science, vol. 150, pp. 482-485.

WOOD, L. E., and THOMPSON, M. C.

1968. Using the geodimeter to measure the refraction correction by dispersion. Final Report, U. S. Army Topographic Laboratories, Fort Belvoir, Virginia, Task I, October.

YEN, J. L.

1968. The Canadian long baseline interferometer system. 1968 NEREM Record. IEEE Catalog No. 68C22-NEREM, pp. 64-65.

VORACHEK, J. J.

1968. Investigation of powered lighter-than-air vehicles. Contract F19628-67-C-0047. Goodyear Aerospace Corporation, Akron, Ohio. Final Report for AFCRL Office of Aerospace Research, U.S. Air Force, Bedford, Massachusetts.